# Emission and Drivability Tradeoffs in a Variable Cam Timing SI Engine with Electronic Throttle

S. C. Hsieh*, A. G. Stefanopoulou†, J. S. Freudenberg*, K. R. Butts†

## Abstract

Tradeoffs between low feedgas emissions and smooth brake torque are discussed in the context of an engine equipped with variable camshaft timing (VCT). The use of VCT lowers the generation of feedgas emissions but adversely affects the torque response. However, with the addition of an electronic throttle and knowledge of online torque, the tradeoffs between emissions and drivability in the VCT engine can be lessened; conventional (non-VCT) engine torque response can be achieved while simultaneously preserving most of the emissions benefits gained by using VCT.

## 1.  Introduction

Previous papers have described the use of variable cam timing (VCT) in a conventional SI engine to reduce HC and NOx feedgas emissions while simultaneously improving fuel economy [4, 6]. It was noted in [4] that there are significant interactions between the performance outputs—torque ($TQ$), cam phasing ($CAM$), and air-fuel ratio ($A/F$). These interactions impose tradeoffs among drivability, feedgas emissions, and catalytic converter efficiency. In particular, the quicker the cam actuator can move, the faster feedgas emissions can be lowered. On the other hand, moving the cam too quickly will result in large deviations from stoichiometric air-fuel ratio as well as hesitation in torque response, both of which are undesirable. The authors in [4] regulate air-fuel ratio using a multivariable controller; the problem of regulating torque response in a VCT engine was not directly addressed.

It has been observed that tradeoffs among drivability, fuel economy, and emissions are less severe with the availability of an electronic throttle [7]. In this paper, we study how this additional actuator, together with an online torque sensor, allow us to preserve the feedgas emissions improvements shown in [4] while maintaining the torque performance of a conventional engine. We will design a $3 \times 3$ multivariable feedback controller to assess the performance improvements afforded by the new actuator and sensor. Our control design expands the usage of retarded cam phasing over a larger operating regime

of the engine to further lower emissions and improve fuel economy.

The term *VCT w/ET* will be used throughout the rest of this paper to represent a VCT engine using an electronic throttle and online torque sensor. *VCT w/MT* denotes a VCT engine using a mechanical throttle linkage, and *conventional engine* refers to an equivalent engine with fixed cam timing and mechanical throttle linkage.

## 2.  Design Objectives

The dual-equal VCT engine model used in this paper is based on the model developed in [4]. It assumes constant engine speed and is open-loop stable due to a built-in feedforward fuel estimator. A controller is needed in order for the VCT engine to achieve the following performance objectives: (i) Maintain the air-fuel ratio close to stoichiometric ratio (14.64 for standard fuel); (ii) Retard the cam phasing to the maximum amount quickly; and (iii) Match the torque response of an equivalent conventional engine with fixed cam timing when possible.

It is important that $A/F$ remains close to stoichiometry in order to achieve high catalytic converter efficiency. The efficiency curves of the three-way catalyst are steep and drop quickly with even the slightest deviations. By keeping catalytic conversion efficiencies at their peak and reducing feedgas emissions, tailpipe emissions are reduced.

The second objective, retarding $CAM$ to the maximum cam retard quickly, is desired so that HC and NOx feedgas emissions leaving the exhaust manifold are minimized. As long as combustion stability is preserved, there is a monotonic relationship between cam and the generation of feedgas emissions; the more the cam is retarded, the less HC and NOx is generated for a given load and engine speed. Furthermore, the intake manifold pressure increases as the cam is retarded due to a decrease in fresh air inducted during the intake stroke. Operation under a higher manifold pressure for a given load translates to higher fuel efficiency [7].

Finally, despite the fact that a dual-equal VCT strategy will affect the cylinder air charge, we would like the torque response of the VCT engine to closely match the torque response of the conventional engine during fast acceleration demands. Any deviation from the conventional engine torque response is undesirable.

## 3. Effects of VCT on Engine Torque

In this section, we illustrate the effects of variable cam timing on torque response. The consequences of a mechanical linkage between the pedal and throttle plate versus an electronic throttle actuator are then discussed.

### 3.1. Torque Response

We begin by writing the nonlinear equations that describe torque generation:

$$\dot{m}_\theta = F_1(P_m, TP) \tag{1}$$

$$\frac{d}{dt}P_m = K_m(\dot{m}_\theta - \dot{m}_{cyl}) \tag{2}$$

$$\dot{m}_{cyl} = F_2(CAM, P_m, N) \tag{3}$$

$$TQ = F_3(\dot{m}_{cyl}, N, A/F) , \tag{4}$$

where $\dot{m}_\theta$ is the mass air flow rate through the throttle body, $\dot{m}_{cyl}$ is the mass air flow rate into the cylinders, $P_m$ is the intake manifold pressure, $CAM$ is the cam phasing, $N$ is the engine speed, $A/F$ the air-fuel ratio, and $TP$ is the throttle angle/position. The functions $F_1$, $F_2$ and $F_3$ are static nonlinear regression maps of engine-dynamometer data [4]. Assuming $N$ and $A/F$ to be constant, $TQ$ depends only on the mass air flow into the cylinders. This assumption is valid during fast throttle movements (torque requests) and allows us to study the effects of the cam timing on engine torque generation considering only the breathing process dynamics.

Linearization of Equations (1)–(4) will further clarify the dynamical characteristics of torque at quasi-static operation:

$$\Delta\dot{m}_\theta = k_{\theta 1}\Delta TP - k_{\theta 2}\Delta P_m \tag{5}$$

$$\frac{d}{dt}\Delta P_m = k_m(\Delta\dot{m}_\theta - \Delta\dot{m}_{cyl}) \tag{6}$$

$$\Delta\dot{m}_{cyl} = -k_{p1}\Delta CAM_{act} + k_{p2}\Delta P_m \tag{7}$$

$$\Delta TQ = k_t\Delta\dot{m}_{cyl} , \tag{8}$$

where $k_{\theta i} > 0$, $k_{pi} > 0$ for $i = 1, 2$, $k_m > 0$, and $k_t > 0$. The transfer function between cam timing, throttle position, and torque response is given by:

$$\Delta TQ(s) = \frac{k_t k_m k_{\theta 1} k_{p2}}{s + k_m(k_{\theta 2} + k_{p2})}\Delta TP(s)$$
$$- \frac{k_t(k_m k_{p1}k_{\theta 2} + k_{p1})s}{s + k_m(k_{\theta 2} + k_{p2})}\Delta CAM_{act}(s) . \tag{9}$$

### 3.2. VCT w/MT Torque Response

In the VCT w/MT engine, the throttle is mechanically linked to the driver's pedal position ($PP$) and controlled by the driver. Hence, $TP = PP$. Since only $CAM$ and fuel injected ($F$) are controllable inputs, the throttle acts as a disturbance to the system. As a result, the torque performance of the engine will be strongly affected by the cam bandwidth and amount of cam retard.

The desired cam phasing is scheduled on pedal position and engine speed ($CAM_{des} = F_4(PP, N)$). If we model the closed-loop cam as a 1st order low-pass filter ($\tau_{vct}\frac{d}{dt}CAM_{act} + CAM_{act} = CAM_{des}$) and linearize the cam scheduling scheme at a constant engine speed ($\Delta CAM_{act}(s) = \frac{k_o}{\tau_{vct}s+1}\Delta PP(s)$)[1], then substitution into Equation (9) yields:

$$\Delta TQ(s) = k_t(k_m k_{\theta 1}k_{p2}\tau_{vct} + k_{p1}k_o)$$
$$\cdot \left[ \frac{s + \frac{k_m(k_{\theta 1}k_{p2} - k_{p1}k_{\theta 2}k_o)}{k_m k_{\theta 1}k_{p2}\tau_{vct} + k_{p1}k_o}}{[s + k_m(k_{\theta 2} + k_{p2})](\tau_{vct}s + 1)} \right] \Delta PP(s) . \tag{10}$$

On the other hand, the transfer function that describes the torque response in the conventional engine during changes in pedal position can be found by linearizing Equations (1)–(4) after setting $CAM = 0$:

$$\Delta TQ(s) = \frac{k_t k_m k_{\theta 1}k_{p2}}{s + k_m(k_{\theta 2} + k_{p2})}\Delta PP(s) . \tag{11}$$

Note that Equation (11) can also be derived from Equation (10) by setting $k_{p1}$ equal to zero.

The torque of the two systems as a function of pedal position behaves considerably differently as the following table shows:

| | Conventional | VCT w/MT |
|---|---|---|
| DC Gain | $\tilde{k}_{dc} = k_t \frac{k_{\theta 1}k_{p2}}{k_{\theta 2}+k_{p2}}$ | $\tilde{k}_{dc} = k_t \frac{k_{\theta 1}k_{p2} - k_o k_{p1}k_{\theta 2}}{k_{\theta 2}+k_{p2}}$ |
| Transfer Function | $\frac{\Delta TQ(s)}{\Delta PP(s)} = \tilde{k}_{dc}\frac{1}{\frac{s}{p_m}+1}$ | $\frac{\Delta TQ(s)}{\Delta PP(s)} = \tilde{k}_{dc}\frac{\frac{s}{z}+1}{(\frac{s}{p_m}+1)(\frac{s}{p_{vct}}+1)}$ |

where $p_m = k_m(k_{\theta 2} + k_{p2})$, $p_{vct} = \frac{1}{\tau_{vct}}$, and

$$z = \frac{k_{\theta 1} - k_o k_{\theta 2}\frac{k_{p1}}{k_{p2}}}{k_{\theta 1}\tau_{vct} - k_o \frac{k_{p1}}{k_m k_{p2}}} .$$

Depending on the steady-state cam schedule ($k_o$) and the speed at which the cam is retarded ($\tau_{vct}$), the location of the extra pole and zero in the torque response of the VCT w/MT engine will vary significantly. Since $k_o$ can be positive or negative, the VCT w/MT torque response may be minimum phase or non-minimum phase. Furthermore, during subsonic flow[2] ($k_{\theta 2} \neq 0$), the steady-state torque will differ between the two engines.

### 3.3. Benefits of Electronic Throttle and Online Torque Measurement

By adding an electronic throttle actuator, the throttle is no longer a disturbance to the system; it can be decoupled from the driver's pedal. Doing so affords more

---

[1] Unlike the other constants, $k_o = \frac{\partial(\text{Cam Schedule})}{\partial TP}$ can be positive or negative.

[2] A more thorough discussion of sonic and subsonic flow across the throttle body can be found in [1].

flexibility in specifying the relationship between engine performance and driver demand.

The availability of an online brake torque measurement then allows the controller to track desired torque using the throttle actuator. Consequently, the torque response of the VCT w/ET engine can be made similar to that of the conventional engine. This was not possible in the case of the VCT w/MT engine because its torque response was determined by Equation (10). To accomplish the task of achieving the steady-state torque of the conventional engine on the VCT w/ET engine, a feedforward schedule will be used in the controller design to map the driver's pedal position into desired torque and cam phasing. Without an online torque measurement, the controller has no way of tracking torque. One could invert the path from throttle to torque in the form of a feedforward controller, but this would require an excellent model of the nonlinear engine.

Although torque measurements are not currently available on mass production vehicles due to cost and robustness issues, studies on torque sensors and torque estimation suggest that such a requirement is not an unrealistic assumption for future vehicles [2]. In this paper, a measurement of torque is assumed to be available.

## 4. Small Signal Analysis of the VCT Model

There are tradeoffs between the objectives listed in Section 2. that must be considered. Of primary importance are the dynamic undesirable dynamic interactions between: (i) the cam phasing to torque and air-fuel ratio, and (ii) throttle to air-fuel ratio. We can examine these interactions by analyzing the $3 \times 3$ open-loop Bode magnitude plot of the VCT engine linearized around two different pedal positions, shown in Figure 1. The commandable inputs to the system are throttle (degrees), cam phasing (degrees), and fuel (g/intake stroke). The measurable outputs are torque (Nm), cam phasing (degrees), and air-fuel ratio (unitless). The $A/F$ measurement was scaled to reflect the importance of small air-fuel ratio deviations from stoichiometry due to disturbances from $CAM$ or $TP$. The fuel input, $F$, was then scaled so that a unit change in fuel resulted in approximately a unit change in the scaled air-fuel measurement. The remaining inputs and outputs were left in engineering units.

In the $P_{12}$ plot of Figure 1, it can be seen that depending on the operating regime, the effect of $CAM$ on $TQ$ may be transient for small pedal angles (sonic flow through the throttle body) or also have a steady state effect for larger pedal angles (subsonic flow through the throttle body). The $P_{21}$ and $P_{23}$ plots are empty because the cam actuator is neither affected by $TP$ nor $F$ in open-loop.

From the $P_{31}$ and $P_{32}$ plots, it is evident that the air-fuel ratio is affected by transient changes in both $TP$ and
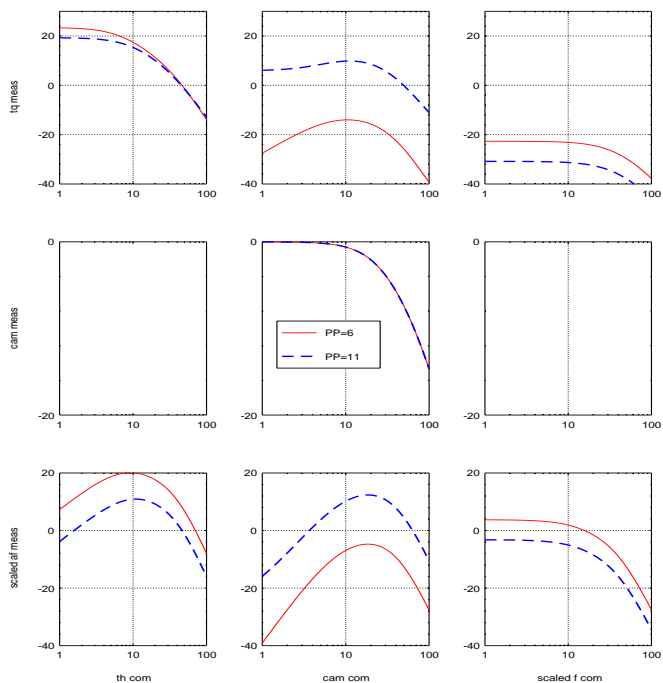


Figure 1: Open-loop Bode magnitude plots (in rad/sec) of the VCT engine at 2000 RPM linearized around PP=6 and PP=11 degrees. The nominal cam input is a function of pedal position to be described in Section 5.1., and the nominal fuel input is 0 g/intake stroke in both cases.

$CAM$. We eliminate the steady-state effects of cam phasing and throttle on air-fuel ratio by using a feedforward fuel estimator based on measured mass air flow across the throttle body. The air-fuel ratio loop bandwidth is limited due to the long delay (720 degrees crank angle) involved—approximately 360 degrees due to combustion and 360 degrees of transport delay—for the exhaust gas to reach the exhaust gas oxygen (EGO) sensor. Therefore, the high frequency disturbances from $TP$ and $CAM$ to air-fuel ratio cannot be effectively attenuated. Note that the magnitude of the $CAM$ disturbance on $TQ$ ($P_{12}$) and $A/F$ ($P_{32}$) also depends on the operating regime. At $PP = 6$ degrees, the magnitude of the disturbances are approximately 20 dB less than at $PP = 11$ degrees.

## 5. Controller Design

The controller used to control the VCT w/ET engine consists of two parts: (i) a static feedforward map from pedal position to desired torque and cam position; and (ii) a linear feedback controller.

### 5.1. Steady-State Feedforward Map

The amount that the cam should be retarded is determined *a priori* and is a function of pedal position and engine speed. We create two feedforward maps: (i) driver's pedal position to desired torque; and (ii) driver's pedal
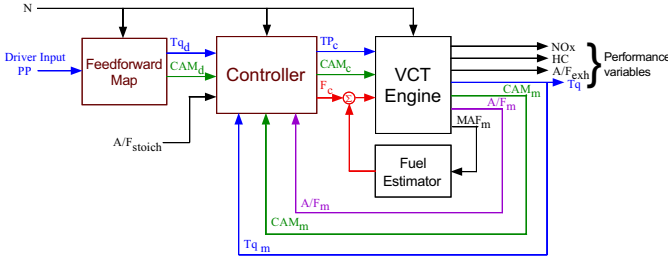
Figure 2: Block diagram of the VCT w/ET controller.

position to desired cam phasing. These maps are coordinated to yield the same steady-state torque as that of a conventional engine.

To generate these mappings, accurate knowledge of the steady-state torque as a function of throttle position and cam retard is required (MBT spark timing and stoichiometric air-fuel ratio are assumed). Figure 3 shows the steady-state torque as a function of throttle position for zero and full cam retard at 2000 RPM. Recall that in both the conventional and VCT w/MT engines, $TP = PP$. The torque curve along which $CAM = 0$ is used to map $PP$ to desired $TQ$. In other words, desired steady-state torque for the VCT w/ET engine is the same as the steady-state conventional engine torque output.
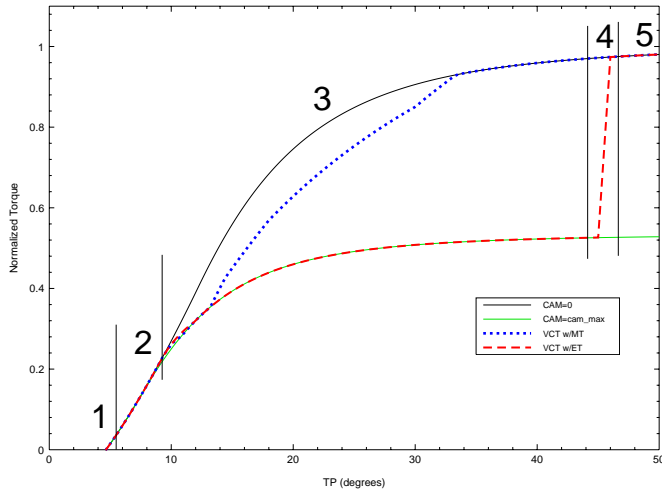


Figure 3: Torque vs. throttle position at 2000 RPM for $CAM = 0$ and $CAM = cam_{max}$.

In order to create a continuous map from pedal position to desired cam phasing, the range of pedal angles is divided into 5 regions (whose boundaries vary with engine speed), also shown in Figure 3. In the first region, cam phasing is fixed at 0 degrees. This way, the VCT engine operates identically to the conventional engine in order to ensure combustion stability. In region two, the cam phasing is progressively retarded from 0 degrees to $cam_{max}$ with increasing $TP$. This region lies within the sonic flow regime, where air flow through the throttle body is a func-

tion of throttle angle only and is not a function of manifold pressure or cam phasing. Thus, we are able to retard the cam without affecting steady-state torque (transient torque *is* affected). In the next region, the cam is kept fully retarded at $cam_{max}$ to get the best emissions and fuel economy benefits from the VCT engine. However, the maximum torque that the VCT engine can generate with retarded cam is much less than the conventional engine. Thus, if the driver demands more torque, it is necessary to advance $CAM$ back to 0 degrees in order to continue increasing torque output, done in region 4. Finally, in region 5 (which extends to wide-open-throttle), $CAM$ is fixed back at 0 degrees and the throttle position follows the pedal position. Here, the VCT engine once again behaves identically to the conventional engine in order to maximize torque output.

## 5.2. MIMO Feedback Controller

LQG methodology was used in the design of the $3 \times 3$ controller in order to specify tradeoffs between the various performance variables (HC, NOx, $TQ$, and $A/F$). In order to ensure steady-state tracking of the reference inputs in the presence of disturbances, the open-loop system was augmented with three integrators (one for each reference signal).

The system was linearized at 2000 RPM with a pedal position of 6 degrees, cam phasing equal to 30% $cam_{max}$, and 0 g/intake stroke fuel. This was the initial operating point studied because it is where the cam is transitioned and is the operating regime most commonly visited. Delays in the nonlinear system were approximated as lowpass filters with the exception of a 2 engine cycle (720 degrees) delay in the $A/F$ loop, which was approximated by a 2nd order Padé approximation.

Closed-loop bandwidth specifications were dictated by performance requirements. The torque bandwidth was chosen so that the VCT w/ET torque response matched the conventional engine torque response, approximately 8 rad/sec. The closed-loop $A/F$ bandwidth is limited by the long combustion and transport delay before the airfuel ratio can be measured; we chose the bandwidth to be 8 rad/sec as well so that the response during torque steps would not be oscillatory. The severity of the $CAM$ disturbance on torque and air-fuel ratio depends on the speed at which the cam is phased. At 2000 RPM, we chose a cam risetime of 2 engine cycles, which corresponds to a bandwidth around 10 rad/sec.

Figure 4 shows a nonlinear simulation of the conventional and VCT w/ET engine performance outputs in response to steps in pedal position. The VCT engines generate significantly lower NOx emissions at all pedal positions as well as lower HC at low manifold pressure. Note that the NOx output of the VCT w/ET engine is slightly higher during the first $PP$ step because the VCT w/ET engine matches the torque response of the conventional

engine, whereas the VCT w/MT engine does not; drivability was not compromised in the VCT w/ET engine. The torque response of the VCT w/MT engine, on the other hand, is noticeably worse for large pedal steps because retarded cam reduces air flow into the cylinder and there is no way in which the VCT w/MT controller can compensate. Both VCT engines also operate at higher manifold pressures than does the conventional engine. This is beneficial to fuel economy due to a reduction in pumping losses [6].
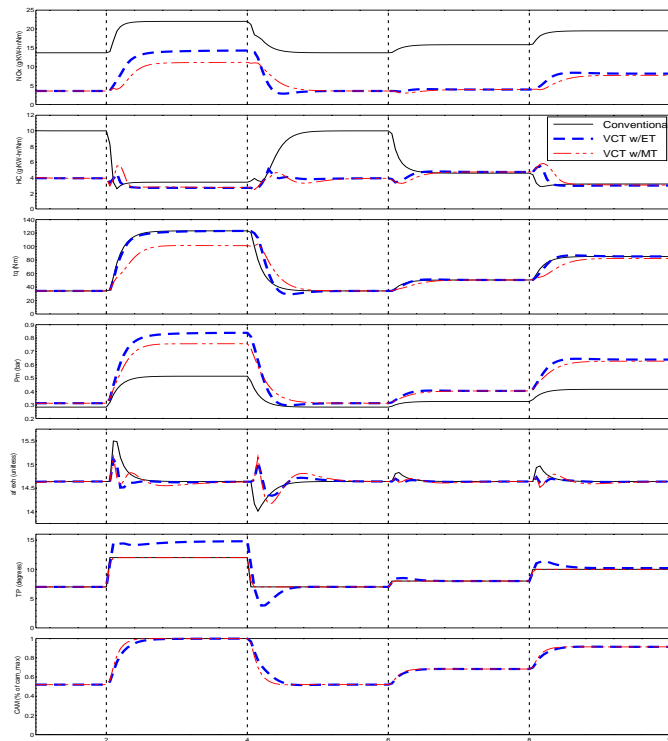


Figure 4: Comparison of the conventional, VCT w/ET, and VCT w/MT engines in response to a series of *PP* steps (12, 7, 8, 10 degrees) at 2000 RPM and cam risetime equal to 2 engine cycles. From top to bottom: NOx, HC, torque, manifold pressure, air-fuel ratio, throttle, and cam phasing.

## 6.    Conclusion

We have described the tradeoffs between feedgas emissions and torque response in relation to cam retard. A noticeable reduction in feedgas emissions is possible in the case of the VCT w/MT engine, but this comes at the cost of not being able to match the torque response of the conventional engine. However, the addition of an electronic throttle and online torque sensor makes the above tradeoffs less severe; the VCT w/ET engine allows us to achieve the torque response of the conventional engine while preserving most of the feedgas emissions benefits gained from the VCT w/MT engine.

We also saw that the VCT engine has significant undesirable cross-coupling interactions between the throttle, cam, and fuel actuators. Feedgas emissions can be reduced faster with higher cam bandwidth, but this will result in a larger disturbance effect on torque response and air-fuel ratio. Hence, the use of a multivariable controller is desirable in order to help reduce these undesirable interactions between the three loops.

Multivariable controller complexity increases with the addition of the electronic throttle actuator and torque sensor. This issue was not addressed in this paper and requires further study. In particular, the closed-loop cam bandwidth can reduce or increase the level of effective coupling between the three loops. Thus, if the closed-loop cam bandwidth is chosen carefully, a full multivariable controller may not be needed; a decentralized controller used to control one or two of the loops may work equally well without any degradation in performance. Simplification of the multivariable controller is highly desirable since it would make implementation of the controller easier. In addition, knowledge of the controller structure will aid in the future work of gain scheduling the controller across different engine speeds and operating regimes.

## References

[1] P. R. Crossley and J. A. Cook, "A Nonlinear Engine Model for Drivetrain System Development," IEE Conference 'Control 91', Edinburgh, U.K., March 1991, IEE Conference Publication 332 Vol. 2, pp. 921-925.

[2] S. Drakunov, G. Rizzoni, and Y. Wang, "On-Line Estimation of Indicated Torque in IC Engines Using Nonlinear Observers," SAE Paper No. 950840.

[3] J. J. Moskwa and J. K. Hedrick, "Modeling and Validation of Automotive Engines for Control Algorithm Development," ASME J. Dynamic Systems, Meas., and Contr., Vol. 114, pp. 278-285, 1992.

[4] A. G. Stefanopoulou, J. A. Cook, J. S. Freudenberg, J. W. Grizzle, M. Haghgooie and P. S. Szpak, "Modeling and Control of a Spark Ignition Engine with Variable Cam Timing," Proc. 1995 Amer. Contr. Conf., pp. 2576-2581, Seattle, 1995.

[5] A. G. Stefanopoulou, K. R. Butts, J. A. Cook, J. S. Freudenberg and J. W. Grizzle, "Consequences of Modular Controller Development for Automotive Powertrains: A Case Study," Proc. 1995 Conf. on Decision and Control, pp. 768-773, New Orleans, 1995.

[6] R. A. Stein, K. M. Galietti, and T. G. Leone, "Dual Equal VCT- A Variable Camshaft Timing Strategy for Improved Fuel Economy and Emissions," SAE Paper No. 950975.

[7] H.-M. Streib and H. Bischof, "Electronic Throttle Control: A Cost Effective System for Improved Emissions, Fuel Economy, and Drivability", SAE Paper No. 960338.